Top Med Chem (2020) 34: 1–32
DOI: 10.1007/7355_2019_86

Published online: 29 February 2020

Fluorescence Molecular Imaging of Medicinal Chemistry in Cancer

Jie Tian, Yang Du, Chu Tang, and Yu An

Contents

J. Tian (✉)
CAS Key Laboratory of Molecular Imaging, The State Key Laboratory of Management and Control for Complex Systems, Institute of Automation, Chinese Academy of Sciences, Beijing, China

Beijing Key Laboratory of Molecular Imaging, Beijing, China

University of Chinese Academy of Sciences, Beijing, China

Beijing Advanced Innovation Center for Big Data-Based Precision Medicine, Beihang University, Beijing, China

Engineering Research Center of Molecular and Neuro Imaging of Ministry of Education, School of Life Science and Technology, Xidian University, Xi'an, Shaanxi, China
e-mail: jie.tian@ia.ac.cn; tian@ieee.org; http://www.3dmed.net

Y. Du and Y. An
CAS Key Laboratory of Molecular Imaging, The State Key Laboratory of Management and Control for Complex Systems, Institute of Automation, Chinese Academy of Sciences, Beijing, China

Beijing Key Laboratory of Molecular Imaging, Beijing, China

University of Chinese Academy of Sciences, Beijing, China

C. Tang
Engineering Research Center of Molecular and Neuro Imaging of Ministry of Education, School of Life Science and Technology, Xidian University, Xi'an, Shaanxi, China

Abstract The process of new drug discovery and development is a lengthy, high-risk, and costly task. Fluorescent molecular imaging (FMI) has tremendous potential for improving the efficiency of drug screening, evaluating drug effects, accelerating the process, and markedly reducing the cost of new drug development from initial target validation and high-throughput screening identification campaigns to the final human translation phases. FMI can help evaluate the role of new candidate drugs under the influence of complex biological responses in living subjects and better understand the mechanism between drug activity and disease, which can help select candidates that seem most likely to succeed or prevent the development of drugs that seem to fail in the end. Hence, in this chapter, FMI was described for its application in drug discovery, including identification of tumor-specific markers, candidate drug screening, determination of pharmacokinetics of drugs, and preparation of prodrugs.

Keywords Cancer, Drug discovery, Fluorescent molecular imaging, Medicinal chemistry

Abbreviations

BBTD	Benzobisthiadiazole
BEM	Boundary element method
BLI	Bioluminescence imaging
BODIPY	Boron dipyrromethene
Cy	Cyanine
D-A-D	Donor-acceptor-donor scaffold
DE	Diffusion equation
FDM	Finite difference method
FEM	Finite element method
FITC	Fluorescein isothiocyanate
FMI	Fluorescence molecular imaging
FMT	Fluorescence molecular tomography
GFP	Green fluorescent protein
HDACs	Histone deacetylases
ICG	Indocyanine green
MM	Meshless method
NIR	Near-infrared
ROS	Reactive oxygen species
SBR	Signal-to-background ratio

1 Introduction

Fluorescence molecular imaging (FMI) utilizes molecular probes to label target organisms. Under certain external conditions, the molecular probe releases a fluorescent light in the visible or near-infrared spectrum using high-sensitivity detection equipment for fluorescence. The signal is collected, and the position and intensity of the fluorescent light source are displayed to obtain the physiological activity information of the organism (Fig. 1). FMI is the most intuitive imaging modality, and the fluorescent methods allow us to detect photons with familiar parallels to our eyesight, allowing spatial and temporal resolutions that are otherwise unachievable [1, 2]. Compared to the positron emission tomography (PET) imaging and magnetic resonance imaging (MRI), FMI is a noninvasive and nonionizing imaging modality with higher sensitivity and higher specificity, is safer, has a lower cost, and is easier to perform, and it offers anatomical, physiological, and even molecular information within the bodies of living subjects [3–5]. Therefore, FMI has been widely applied for tumor detection, drug development, image-guide surgery, and other biomedical fields.

From a medicinal chemistry perspective, FMI is a potent tool for probing biomolecules in their natural environment and for visualizing dynamic processes in complex biological samples, living cells, and organisms [6–9], which are well suited for highlighting molecular alterations associated with pathological disorders. Thereby, it offers means of implementing sensitive and alternative technologies for diagnostic purposes, which constitute as attractive tools for drug discovery programs from initial target validation and high-throughput screening identification campaigns to the final clinical translation phases. In this chapter, the FMI probe, imaging analysis methods, and medical application in drug discovery will be described.

2 Imaging Probe

Fluorescence probe is one of the basic elements of FMI. Fluorescence probes are usually made up of fluorophores and targeting ligands.

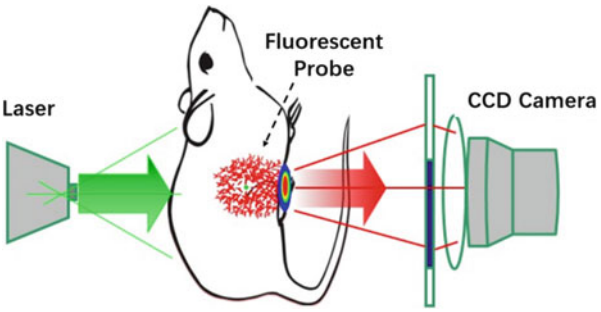

Fig. 1 The principle of fluorescence molecular imaging (FMI)

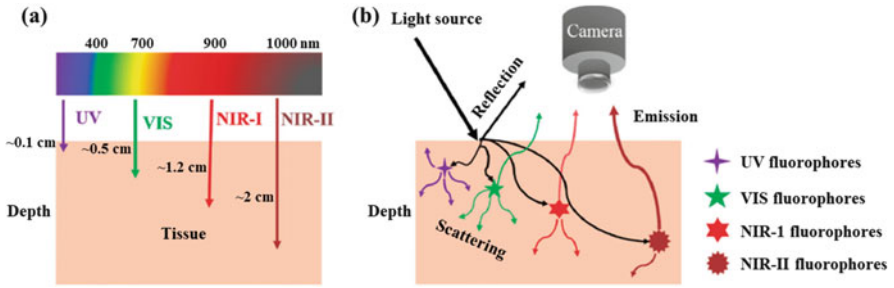

Fig. 2 Wavelengths for fluorescence molecular imaging. (**a**) Tissue penetration depth of light with different wavelengths. (**b**) Light when entering a tissue can be reflected or adsorbed by molecules within the tissue or excite fluorophores to emit light at a different wavelength. Reproduced from Ref. [11]

2.1 Fluorophores

The fluorophore can convert molecular recognition information into a fluorescence signal, which has the advantages of high sensitivity, rapid reaction time, and the ability to realize in situ detection. An ideal fluorophore has a large value of Stokes shift [difference between the absorption maximum (λ_{max}) and the emission maximum (λ_{em})] to minimize the reabsorption of emitted photons. According to the fluorophore with emission in different regions, it can be divided into three categories: visible light ($\lambda_{em} < 700$ nm), near-infrared I (NIR-I, $700 < \lambda_{em} < 1{,}000$ nm), and near-infrared II (NIR-II, $\lambda_{em} > 1{,}000$ nm) fluorophores (Fig. 2) [10, 11].

2.1.1 Visible Light Imaging Fluorophores

Visible light fluorophores mainly include fluorescein isothiocyanate (FITC), cyanine (Cy), rhodamine, BODIPY, coumarin, quinoline, etc. (Fig. 3) [12–16]. These fluorophores are fluorescent indicators with rapid detection, good reproducibility, and low sample size, which can be used to detect the changes of cations (Na^+, K^+, Mg^{2+}, Ca^{2+}, etc.), anions (phosphate radical, etc.), free radicals (reactive oxygen species H_2O_2, superoxide ion), monolinear oxygen, hydroxyl radical, sugar (glucose, chitosan, etc.), nucleic acid (DNA, RNA), and enzymes (trypsin, viral protease, no synthase) in biological systems after drug therapy [17–19]. The visible light fluorophores (400–700 nm) are used quite often in biomedical studies, but the key issues in fluorescence imaging of visible regions include autofluorescence, quenching, photobleaching, and a low depth of tissue penetration. In comparison, fluorescence imaging in NIR offers considerable advantages. However, the use of NIR fluorophores requires a special camera, as the light is not visible to the naked eye or conventional video cameras.

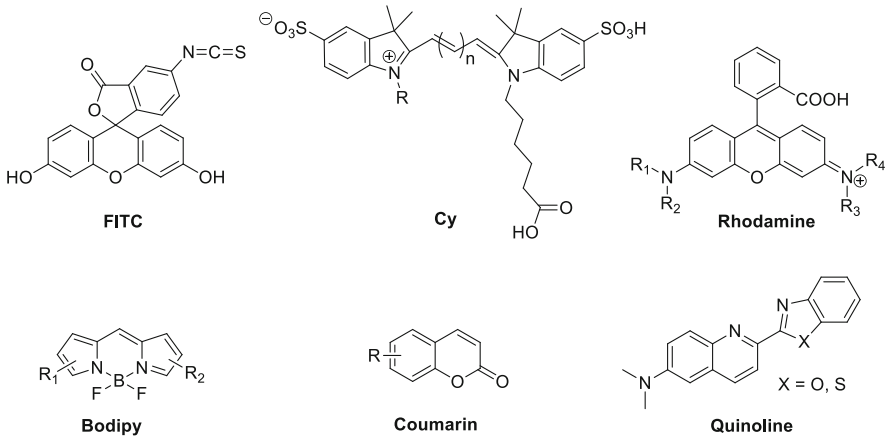

Fig. 3 Representative visible light fluorophores

Fig. 4 Representative NIR-I fluorophores

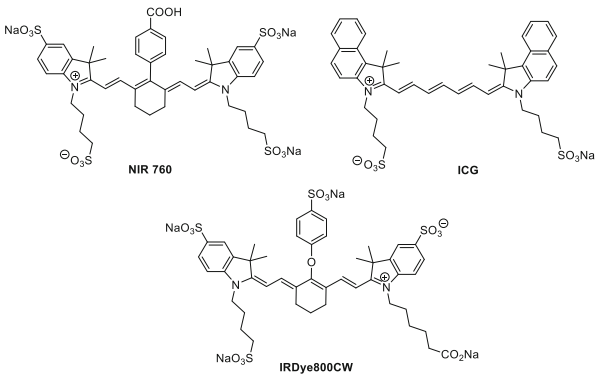

2.1.2 NIR-I Imaging Fluorophores

Fluorophores with emission in the NIR region possess less absorption and scatter from tissues much more efficiently than fluorophores based on visible light, which is favorable for in vivo imaging with a high signal-to-background ratio (SBR). This imaging modality also inherited quick feedback, high-resolution, and noninvasive properties of optical imaging and can be utilized to visualize the real-time dynamics in living organisms [20–23]. Over the past decade, fluorescence imaging in the first NIR window (NIR-I, 700–900 nm) has been widely studied in fundamental research and preclinical/clinical applications, which is partially because of the immediate availability of a wide range of fluorophores, such as NIR-760, IRDye800CW, indocyanine green (ICG), methylene blue, and their derivatives (Fig. 4) [24–26].

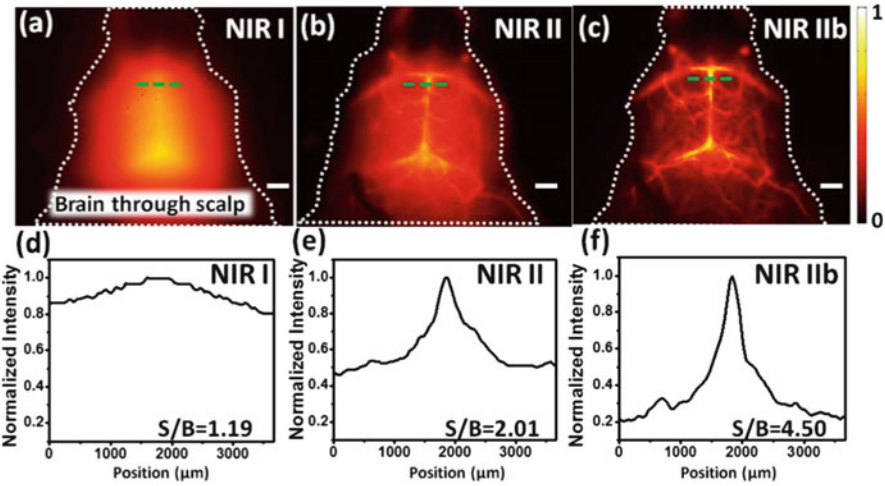

Fig. 5 Fluorescence imaging of the cerebrovasculature of mice without craniotomy in the (**a**) NIR-I, (**b**) NIR-II, and (**c**) NIR-IIb regions, with the corresponding SBR analysis shown in (**d**)–(**f**). Scale bars, 2 mm. Reproduced from Ref. [30]

2.1.3 NIR-II Imaging Fluorophores

The generation of new fluorophores and the development of fluorescent labeling technology provide specific and efficient contrast for FMI and greatly improve the detection sensitivity and specificity of in vivo imaging. Compared to NIR-I, fluorescence imaging at the second near-infrared region (NIR-II, 1,000–1,700 nm) can realize better fluorescence image quality (Fig. 5) [27]. The NIR-II biological window is broadly defined as wavelengths in range of 1,000–1,700 nm. Smaller optical sub-windows such as NIR-IIa (1,300–1,400 nm) and NIR-IIb (1,500–1,700 nm) have provided further improvements in fluorescence imaging metrics. The 1,400–1,500 nm window is typically avoided owing to the presence of an absorbance peak due to a water overtone. Significant improvements in imaging temporal and spatial resolution (~20 ms and ~25 μm) and penetration depth (up to ~3 cm), which are very difficult to achieve with NIR-I and also PET and SPECT imaging, have been fulfilled by this innovative NIR-II region on biomedical imaging, thanks to the reduced scattering, negligible tissue absorption, and minimal autofluorescence [28, 29].

However, NIR-II fluorophores also suffer from poor water solubility, low photostability, low quantum yield, and the scarcity of molecules with suitable NIR-II band gaps have further limited the applications and development of NIR-II imaging techniques. So far, a series of fluorophores with emission wavelengths longer than 1,000 nm in the NIR-II region have been designed based on the donor-acceptor-donor scaffold (D-A-D). These NIR-II fluorophores are usually composed of various spacers (thiophene), electron donor (fluorene and triphenylamine), and the central electron-accepting aromatic backbone (benzobisthiadiazole, BBTD), which can greatly expand the library of small-molecule NIR-II fluorophores (Fig. 6) [31–33]. Fortunately, a series of organic small molecules and organic and inorganic nanomaterials with precisely

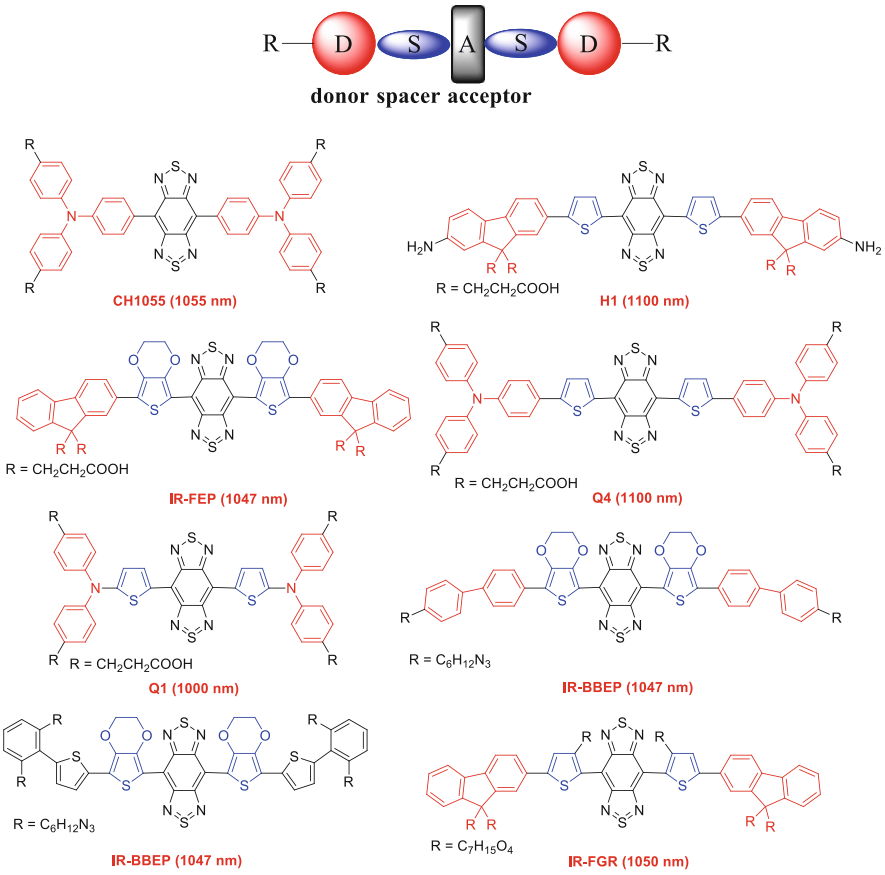

Fig. 6 Representative NIR-II fluorophores

controlled structures and intrinsic near-infrared emissions in the NIR-II window have been developed to enable the acquisition of high-definition NIR-II images at wavelengths well in excess of 1,000 nm. These NIR-I and NIR-II fluorophores can be used to develop diagnostics, biomedical imaging technologies, and drug discovery programs.

2.2 Targeted Ligand of Fluorescent Probes

In the field of medicinal chemistry, the target is the key element for the drug design and development. FMI has the advantages of high sensitivity, convenience, reliability, and suitability for large-scale detection of drug targets. Using FMI, not only the receptors, proteins, and genes that interact with drugs can be imaged, but the drug targets can also be located and evaluated for their presence in an organism. The spatial and temporal distribution of the target is evaluated quantitatively. Verification

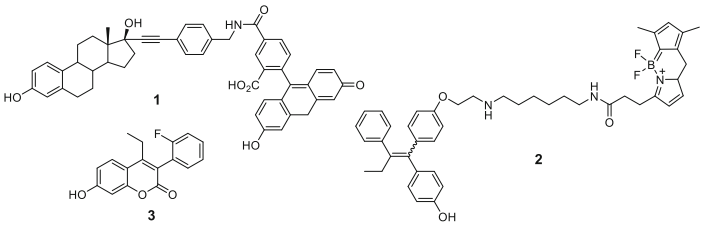

Fig. 7 Representative estrogen receptor-targeted fluorescent probes **1**–**3**

of target expression is valuable for diagnosis, as well as the selection of treatment regimen and pre-evaluation. There are often overexpressed specific receptors on the surface of tumor cells. For example, abnormal overexpression of estrogen receptor (ER) [34–36] and fructose transporter (GLUT5) [37] has been found in breast cancer; prostate-specific membrane antigen (PSMA) is overexpressed in prostate cancer [38–41]. FMI can be used to determine the expression level of related hormone receptors in tumor biopsy specimens, which can help select the best treatment plan. Using these receptors as targets to develop new, potential drugs with high specificity and affinity is the main direction of development of antitumor drugs. Currently, many active targeted fluorescence probes have been developed.

2.2.1 Estrogen Receptor-Targeted Fluorescent Probes

Estrogen receptor (ER) is a ligand-regulated transcription factor that regulates many physiological and pathological processes and also plays a predominant role in breast cancer growth. Therefore, ER is regarded as an important pharmaceutical target for the treatment of breast cancer, and the development of ER-targeted fluorescence probes has emerged as an active research field for breast cancer detection, and many of these probes have been developed (compounds **1**–**3**, Fig. 7) [34–36].

2.2.2 GLUT5 Transporter-Targeted Fluorescent Probes

Facilitated hexose transporters (Gluts) are a group of transmembrane proteins responsible for transporting sugars such as glucose or galactose across the cell membrane. Tumor cells usually overexpress the Glut transporter to meet their high levels of energy consumption needs. For example, GLUT5 is overexpressed in breast cancer cells but not in normal breast cells. Therefore, the selection of a high GLUT5-binding affinity compound as the targeting ligand is an effective strategy for the development of imaging probes for breast cancer detection (compounds **4**–**5**, Fig. 8) [37].

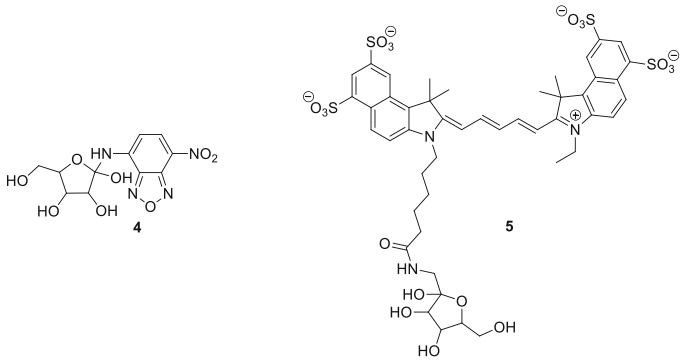

Fig. 8 Representative GLUT5 ligand **4** and targeted fluorescent probe **5**

2.2.3 Prostate-Specific Membrane Antigen (PSMA)-Targeted Fluorescence Probes

Prostate cancer is the most commonly diagnosed malignancy in men, and the integral membrane protein PSMA is becoming increasingly recognized as a viable target for prostate cancer diagnosis and treatment. Therefore, PSMA-specific antibodies, peptides, peptide derivatives, or other small molecules have been developed as targeting ligands for the development of imaging probes for prostate cancer detection (compounds **6**–**9**, Fig. 9) [38–41].

2.2.4 Folate Receptor-Targeted Fluorescent Probes

Folates are essential for the maintenance of all cells and tissue regeneration. Folates have a high affinity for their cell surface folate receptor (FR), which is primarily expressed on healthy cells where it does not readily encounter folate from the bloodstream. When the malignant transformation occurs, high levels of FR are expressed in a number of malignancies, including ovarian and endometrial cancers and myeloid leukemias. Thus, the high affinity of FR offers a potential means for tumor targeting, which has already become the main design strategy for the FR-targeted tumor imaging probes (compounds **10**–**11**, Fig. 10) [42, 43].

2.2.5 Cyclooxygenase-2 (COX-2)-Targeted Fluorescent Probes

COX-2 is a crucial biological mediator in the etiology of cancer. This enzyme is absent or present at low levels in normal cells but shows high expression levels in inflamed tissues as well as many premalignant and malignant tumors such as colorectal adenomas and adenocarcinomas. COX-2 has been used as an ideal imaging biomarker for cancer cells. Currently, many fluorescent probes have been engineered to target COX-2 for tumor detection (compounds **12**–**15**, Fig. 11) [44, 45].

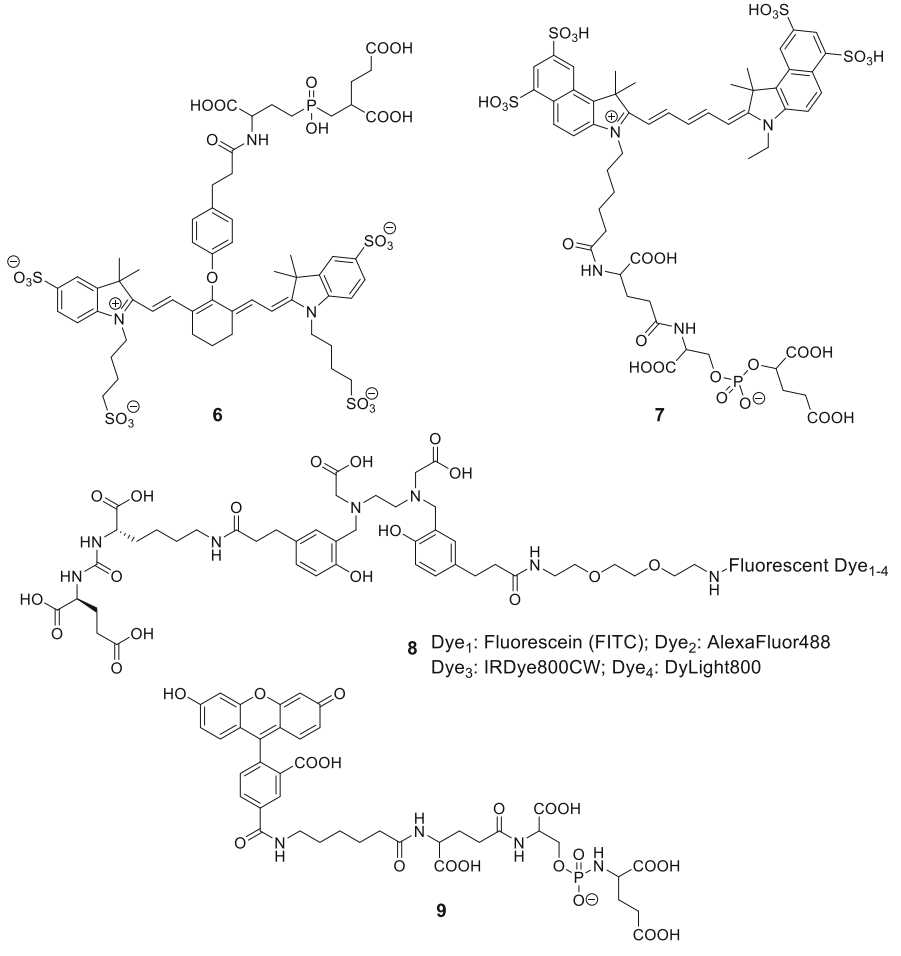

Fig. 9 Representative PSMA-targeted fluorescent probes **6–9**

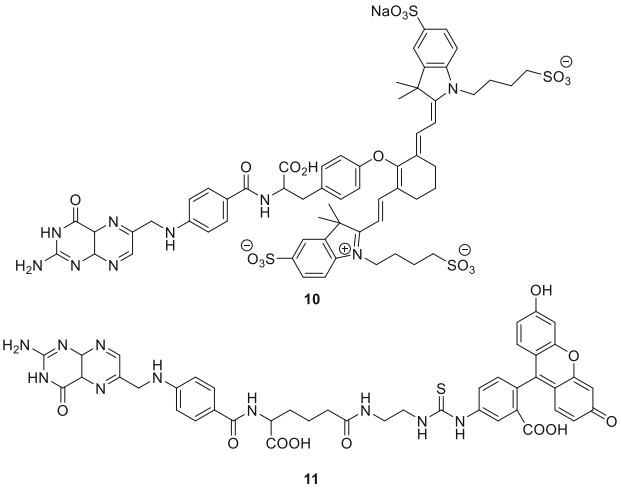

Fig. 10 Representative folate receptor-targeted fluorescent probes **10–11**

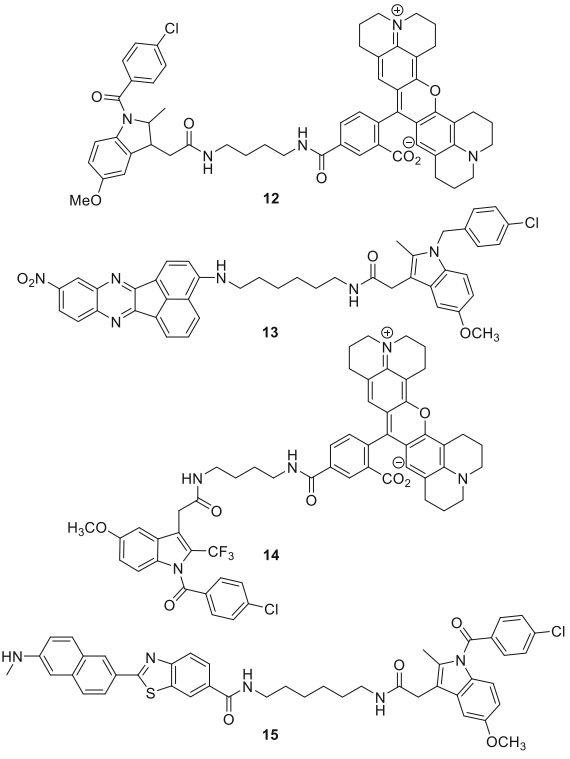

Fig. 11 Representative COX-2-targeted fluorescent probes **12–15**

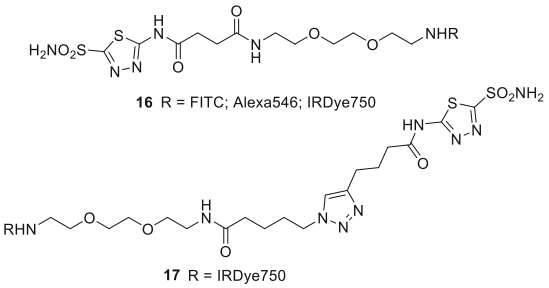

Fig. 12 Representative CAIX-targeted fluorescent probes **16–17**

2.2.6 Other Targeted Fluorescent Probes

In addition to the targeted fluorescence probes mentioned above, various other targeted fluorescence probes have also been reported, such as carbonic anhydrases IX (CAIX) probes. CAIX has been associated with tumor progression and invasion, which is usually expressed in normal tissues at certain levels, but overexpressed in many solid tumors, such as colorectal tumors. Therefore, CAIX can be used as a potential tumor target for the development of imaging probes (compounds **16–17**, Fig. 12) [46, 47].

In general, the targeted fluorescent probes were accomplished by conjugating fluorescence dye to the targeted ligand, which may have a great application prospect in the clinic for tumor diagnosis.

3 Imaging Analysis

Fluorescence molecular tomography (FMT) is a three-dimensional imaging method based on FMI, which is based on the distribution of fluorescence in biological tissues [48–53]. It was developed from two-dimensional (2D) qualitative imaging to three-dimensional (3D) quantitative research and further expanded the integration of stimulated fluorescence in the diagnosis and treatment of cancer and preclinical and clinical applications. The advent of FMT led to the three-dimensional reconstruction of FMI agent accumulation in living animals based on light recordings collected at the tissue boundary. FMT has been used to visualize and quantitate a variety of cellular and molecular events and, as opposed to planar fluorescence imaging, yields quantitative information and allows imaging at greater depth, up to several centimeters. It has developed rapidly in recent years and has become a research frontier and research hotspot for FMI technology [54–56].

When imaging spatial data needed for FMT reconstruction are obtained, then the reconstruction of the structural data and optical data based on the biological model can be carried out [57]. In general, the image reconstruction process includes two steps: solving the forward problem and solving the inverse problem. The solution of

the forward problem is used to calculate the photon propagation model of the fluorescence transmitted in the imaging space to obtain the linear relationship between the fluorescence measurement data on the surface of the tissue and the fluorescence distribution inside the bio-tissue. After the linear relationship is obtained by solving the photon transfer model, various methods are used to solve the linear model, and the distribution of fluorescence inside the imaging space is obtained, which is called the inverse problem [52].

3.1 Photon Propagation Model

The process of transmitting fluorescence from a light source to a biological body through a specific biological tissue is extremely complicated and includes various physical processes such as scattering of light, inter-tissue reflection, refraction, diffusion, and absorption. For FMT imaging, imaging is usually performed in the visible and near-infrared optical bands, and the scattering and absorption effects of this band of light inside the biological tissues are the main forms of our study. Therefore, the FMT photon propagation model can be simplified to a photon stochastic propagation model that contains only the scattering and absorption effects without considering the reflection and refraction of different tissues. Current mainstream mathematical theory to solve these problems is mainly based on Boltzmann's radiative transfer equation (RTE) [58], which is equivalent to photon propagation as transport of photon flux in a medium from particle fluctuation to energy transport and to study transport of light energy in biological tissue problems.

In three-dimensional biological tissue, the RTE solution is transformed into a six-dimensional space-time problem. There are few methods in solving mathematical and computer problems, and they are usually not able to directly close the analytical solution. Moreover, because of its unknowns, it can be solved precisely only in rare cases. Usually it cannot get a closed analytical solution. At the same time, it is extremely difficult to solve RTE directly, while the exact solution will only exist in rare cases. Therefore, it is common practice to replace itself with a simplified approximation of the radiation transfer equation [59], such as diffusion equation (DE), which is a widely used RTE-based simplified model [60–65]. It utilizes the first-order spherical harmonic function to expand important function items in the RTE equation and performs the approximate processing, which significantly reduces the computational complexity and is suitable for the visible and near-infrared bands of FMT imaging. In recent years, researchers have proposed such high-order approximations as RTE [66–71]. Compared with diffusion equations, higher-order approximation models can significantly improve FMT accuracy. The SN model [72], PN model [73], and SPN model [69] are three commonly used RTE high-order approximation models and usually give more accurate RTE solutions to the more diffusive equations. By these approximation methods, the traditional RTE equation can be transformed into several coupled higher-order partial differential equations for easy calculation and solution.

3.2 Forward Problem-Solving

The linear relationship between the measured data on the surface of the imaging area and the internal fluorescence distribution in the imaging area based on the photon propagation model is the core of the FMT forward problem. In recent years, researchers have proposed various mathematical solution methods including the analytic method, statistical method, and numerical analysis method to solve the forward problem of FMT [52]. Numerical analysis method is the main solving method currently used in optical molecular imaging reconstruction. Its computational efficiency is high and its applicability is wide. Numerical analysis methods include the finite difference method (FDM) [70], boundary element method (BEM), finite element method (FEM) [74], and meshless method (MM) [75]. FDM uses equidistant grid points and regular grids to solve the forward problem, which is more efficient than irregular grids. However, FDM has difficulty in dealing with geometrically complex imaging spaces and boundary conditions. In contrast, FEM is the mainstream solution to FMT forward problems in recent years. The main advantage of FEM is its effectiveness in dealing with complex geometric problems. In addition, the system matrices obtained by FEM are usually sparse and positive definite, which leads to a more stable solution and high computational efficiency, which is also beneficial to FMT reconstruction [76, 77]. However, the main drawback of FEM is that it is difficult to generate the FEM grid. In contrast, BEM only needs to discretize the imaging surface and the boundaries of the heterogeneous tissue within the space without the need to mesh the entire imaging space. Therefore, compared with FEM, BEM can effectively reduce the computational dimension and complexity to improve computational efficiency. However, fast and stable 3D mesh generation for complex geometry problems remains a challenging issue. In order to overcome the problem of 3D mesh generation, An et al. proposed a meshless method and applied it to solve the forward problem of FMT [78]. The method only needs to obtain nodes that are relatively independent from each other to discretize the imaging space and does not require a cumbersome gridding process.

3.3 Inverse Problem-Solving

In FMT preclinical and clinical trials, the fluorescence signal is usually only measured from the imaging surface. However, the dimension of the measurement data on the imaging space surface is usually much less than the number of internal nodes in the imaging space. Therefore, the inverse problem of FMT is ill-conditioned [55]. Moreover, because of the high scattering properties of photons in the imaging space, the inverse problem is also ill-posed, and it is difficult to find the exact solution [79–81]. At the same time, the noise generated during the experiment also affects the accuracy of the FMT reconstruction [82].

The ill-posedness of the FMT inverse problem is mainly due to the lack of information and uncertainty due to the high scattering of photons. In order to overcome the ill-posedness of reverse problems, researchers started from the light source prior information and combined it with a variety of a priori information related to the light source and photon transmission to reduce the uncertainty of the information so as to improve the accuracy of inverse problem-solving [83–89]. Researchers usually combined the prior information of the structure into the FMT reconstruction and proposed a nonhomogeneous imaging space model and a priori reconstruction method, which greatly improved the reconstruction accuracy. The structure of imaging space prior information can usually be obtained by high-resolution structural imaging modalities such as CT and MRI [90–94]. The optical parameters of various organs and tissues can be obtained by other imaging techniques such as DOT. The imaging technique that combines imaging modalities to increase imaging prior information is also known as multimodality imaging and is the focus of current medical imaging research [95].

Although researchers have put forward prior knowledge such as feasible regions, structural prior information to augment the information needed for reconstruction, the morbidity of the FMT reconstruction equation remains unresolved. Moreover, the actual FMT acquisition data usually contain a certain amount of noise, which has a great impact on the reconstruction of the pathological equation. A small signal disturbance may lead to a large reconstruction error. Therefore, researchers apply regularization techniques to FMT reconstruction to constrain the reconstruction process and reduce morbidity [96–104]. The classical regularization term is Lp-norm regularization. The Lp-norm regularization ($p = 0.5$–2) usually obtains a smoother reconstructed result of a large reconstructed area and has a good reconstruction effect for a large light source volume in an imaging space. Another available regularization method is total variation (TV) [105]. The main idea of TV norm regularization is to constrain the variation terms of the distribution of the fluorescent light sources while preserving the boundaries of the light source zones (Fig. 13).

4 Medical Application

Precision medicine has promoted the development of treatment modalities that are developed to specifically kill tumor cells but not normal cells. The traditional methods of drug discovery have many disadvantages, such as a long research period and the antitumor drug treatment effects in situ cannot be monitored in real time. Therefore, the use of new technologies such as FMI for drug discovery is urgently needed. It seems likely that FMI will meet this challenge for the evaluation of therapeutic effects. The results were more accurate and reliable than the traditional measurement of tumor size. In this chapter, the application of FMI will be described in drug discovery, including identification of therapeutic targets, candidate drug screening, pharmacokinetics of drugs, and prodrug development.

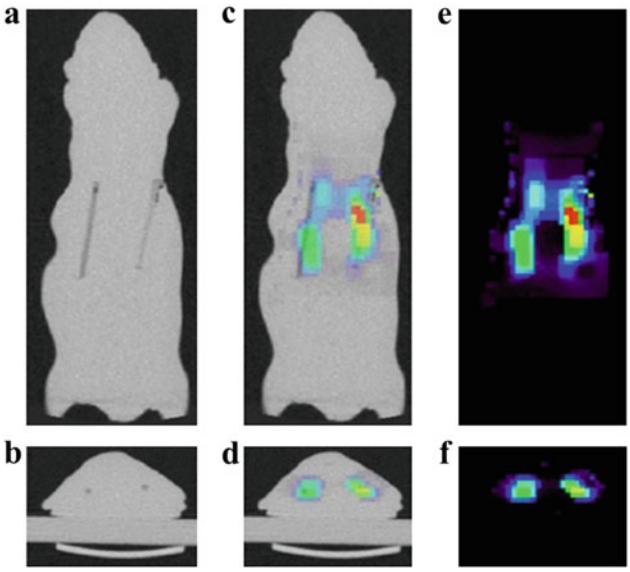

Fig. 13 (**a**) Coronal and (**b**) transverse sections of the CT image of the mouse-shaped phantom showing the two embedded fluorescent line sources. (**c**) Coronal and (**d**) transverse overlay of CT and FMT images. (**e**) Coronal and (**f**) transverse sections of the FMT imaging showing the two fluorescent line sources reconstructed using both L1 and TV penalties with regularization parameters of 10 and 1, respectively. The figure is reproduced from Ref. [105]

4.1 Identification of Therapeutic Targets

Specific therapeutic target is the key for therapy, but traditional drug chemistry methods find targets at slow speed. FMI can improve the process of target identification and identify suitable treatment regimens, hence improving patient treatment outcomes. For example, breast cancer is the most common cancer among women with different subtypes. Nearly 75% of patients demonstrate abnormally high expression of ERα. Therefore, ERα is regarded as an important pharmaceutical target for the treatment of breast cancer, and many ERα ligands have been developed into hormone agents. However, hormone therapy is ineffective for ERα(−) and triple-negative breast cancers (TNBCs). The ERα fluorescent probe P1 can be used to identify a suitable therapeutic regimen for breast cancer. As shown in Fig. 14, the fluorescence signals can be observed in the cell nucleus of the ERα-positive MCF-7 breast cancer cell, but not in MDA-MB-231 TNBC cells. Therefore, FMI is able to identify the target expression and determine treatment [45].

4.2 Candidate Drug Screening

To evaluate the therapeutic effects of antitumor drugs in vivo, a traditional medical imaging method is used to measure the tumor volume at the late stage of tumor

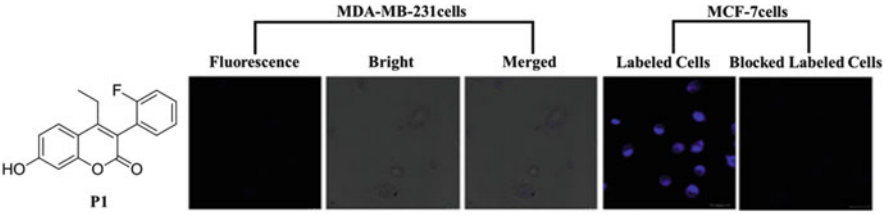

Fig. 14 Fluorescence imaging of intracellular targets in triple-negative breast cancer cells MDA-MB-231 and ER(+) MCF-7 cells. Images of cells treated with compound P1. Reproduced from Ref. [44]

growth with treatment for a period of time. However, this method can only tell the changes in tumors when they show anatomical changes; in addition, it is difficult to evaluate the effect of in situ tumor therapy by the traditional method. FMI can completely overcome the shortcomings of the traditional method and can not only monitor the changes of the tumor biomarker but also evaluate the therapeutic effect in an early and dynamic manner. For example, histone deacetylases (HDACs) are overexpressed in TNBC. The FMI of the LBH589-Cy5.5 probe has been successfully applied not only for measuring the expression and functions of HDACs in tumors but also in evaluating the therapeutic response of HDAC inhibitor SAHA treatment, as evidenced by the significantly reduced HDAC signals in SAHA-treated breast tumors (Fig. 15) [106].

4.3 Tracking the Drug Biodistribution and Metabolism

When the tumor cells were treated with drugs, it was difficult to observe the drug interaction with the corresponding targets by traditional pharmacochemical methods. The majority of drugs tested clinically exhibit off-target effects, which is easy to produce side effects. FMI is able to directly visualize the binding of the drug to the target, which can effectively improve the success rate of drug development. For example, 2-((3-(3-fluoro-4-hydroxyphenyl)-7-hydroxynaphthalen-1-yl) methylene) malononitrile (FPNM) can potently inhibit the growth of MDA-MB-231 tumors, and the relative binding affinity (RBA) value shows FPNM is an estrogen receptor β (ERβ) ligand. In order to confirm the interaction between FPNM and ERβ, FMI of FPNM is performed in MCF-7 cells. As shown in Fig. 16, ERβ is a nuclear hormone receptor, and the fluorescence derived from the complex between FPNM and ERβ was mainly detected in the cell nucleus. The data suggested that FPNM showed specifically selective affinity toward ERβ in the living MCF-7 cells. These results indicated that FPNM possesses the ability to selectively bind to the ERβ in living cells [107].

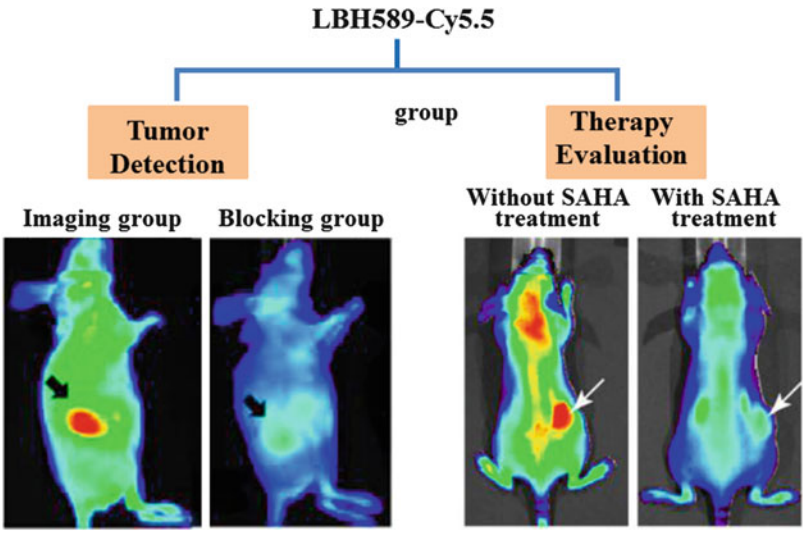

Fig. 15 Detection of tumor and evaluation of antitumor activity of drugs by FMI. Reproduced from Ref. [106]

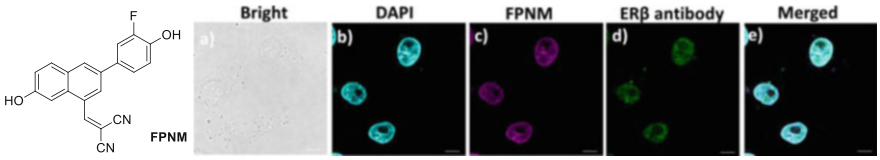

Fig. 16 Co-localization of MCF-7 cells with FPNM (10.0 μM) and ERβ antibody. (**a**) Bright field of cells. (**b**) Nuclei were stained with DAPI. Cells were stained with FPNM (**c**) and ERβ antibody (**d**). Co-localization of FPNM and ERβ antibody. Scale bar = 10 μm. Reproduced from Ref. [107]

4.4 Determination of Pharmacokinetics of Drugs

Targeting specific, small molecules as modulators of drug delivery may play a significant role in the development of therapeutics. Small molecules can alter the pharmacokinetics of therapeutic macromolecules leading to more efficient drug delivery with less systemic toxicity. McCann et al. used FMI to observe the biodistribution and excretion patterns associated with molecular probes composed of human serum albumin (HSA) conjugated to high and low numbers of various monosaccharides: Glc-α, Gal-β, Man-α, Fuc-α, and Fuc-β. First, the conjugation of IRDye800CW to HSA demonstrated nonspecific distribution throughout the body, suggesting the addition of IRDye800CW minimally changed the biodistribution of HSA. However, the conjugation with either low numbers or high numbers of sugar molecules resulted in rapid and specific changes in biodistribution. The conjugation of HSA to a low number of sugar molecules leads to slower clearance of the probe from the blood circulation compared to HSA conjugated to a high number of sugar molecules (Fig. 17) [108].

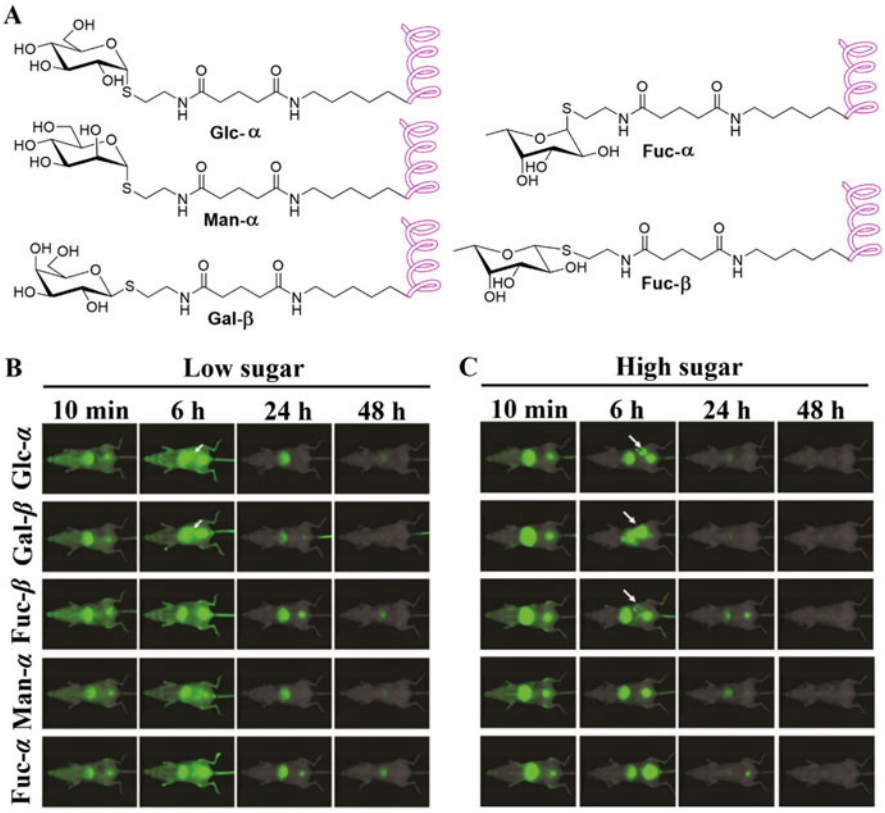

Fig. 17 Chemical structure of the linkage between sugar and albumin. (**a**) the images of HSA glycosylated with a low (**b**) and high (**c**) sugar number at different time points as 10 min, 6 h, 24 h, and 48 h post-injection. Reproduced from Ref. [108]

4.5 Fluorescence Prodrug Conjugates

Fluorescence prodrug conjugates are dual functional systems that offer both therapeutic promise and potential for concurrent diagnosis, which are able to target cancer cells selectively, provide cytotoxic chemotherapeutics, and allow facile monitoring of the location and efficacy of drugs [109, 110]. Fluorescence prodrug conjugates are of particular interest since they are stable in blood plasma, which can be activated efficiently by various cellular constituents, such as thiols, reactive oxygen species (ROS), and enzymes that are overexpressed in tumors [111, 112].

Fluorescence prodrug conjugates can realize both targeted therapeutic release and targeted FMI. Such prodrug conjugates usually contain fluorophores, cleavable linkers, and targeting ligands or chemotherapeutic agents. Fluorophores are usually naphthalimide, coumarin, BODIPY, rhodol, cyanine, etc. Cleavage linkers include hydrolysis of esters, amides, and hydrazine linkers, disulfide exchange-based

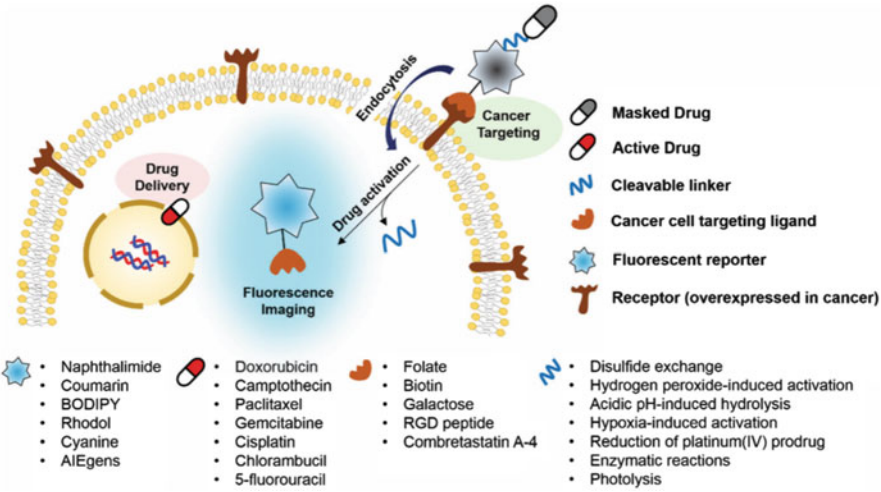

Fig. 18 Design principle for achieving fluorescent prodrug conjugates that are able to target cancer cells selectively, provide cytotoxic chemotherapeutics, and produce readily monitored imaging signals. Reproduced from Ref. [114]

scission, hypoxia-induced activation, enzymatic reactions, photolysis, and thermolysis [113]. Targeting ligands include folate, biotin, galactose, and RGD (Arg-Gly-Asp) peptide sequences. Doxorubicin, camptothecin, paclitaxel, gemcitabine, and cisplatin are commonly used chemotherapeutic agents. To date, much effort has been devoted to develop systems that undergo cleavage under physiological conditions. When the cleavable linkers serve to tether a fluorophore to a prodrug in such a way that the fluorescence signal can be controlled upon cleavage, it becomes a potential system that operates as both therapeutics and diagnostics (Fig. 18) [114].

To date, many fluorescence prodrug conjugates have been reported, including cellular thiol-activatable fluorescent prodrugs (compound **18**) [114], hydrogen peroxide-activated fluorogenic prodrugs (compounds **20**–**21**) [115, 116], acidic pH-activated fluorogenic prodrugs (compounds **22**–**23**) [117, 118], hypoxia-activated fluorogenic prodrugs (compound **24**) [119], platinum reduction-based fluorogenic prodrugs (compound **28**) [120], enzymatic cleavage-based fluorogenic prodrugs (compound **29**) [121], light-activated fluorogenic prodrugs (compounds **32**–**33**) [112, 122], etc. (Fig. 19).

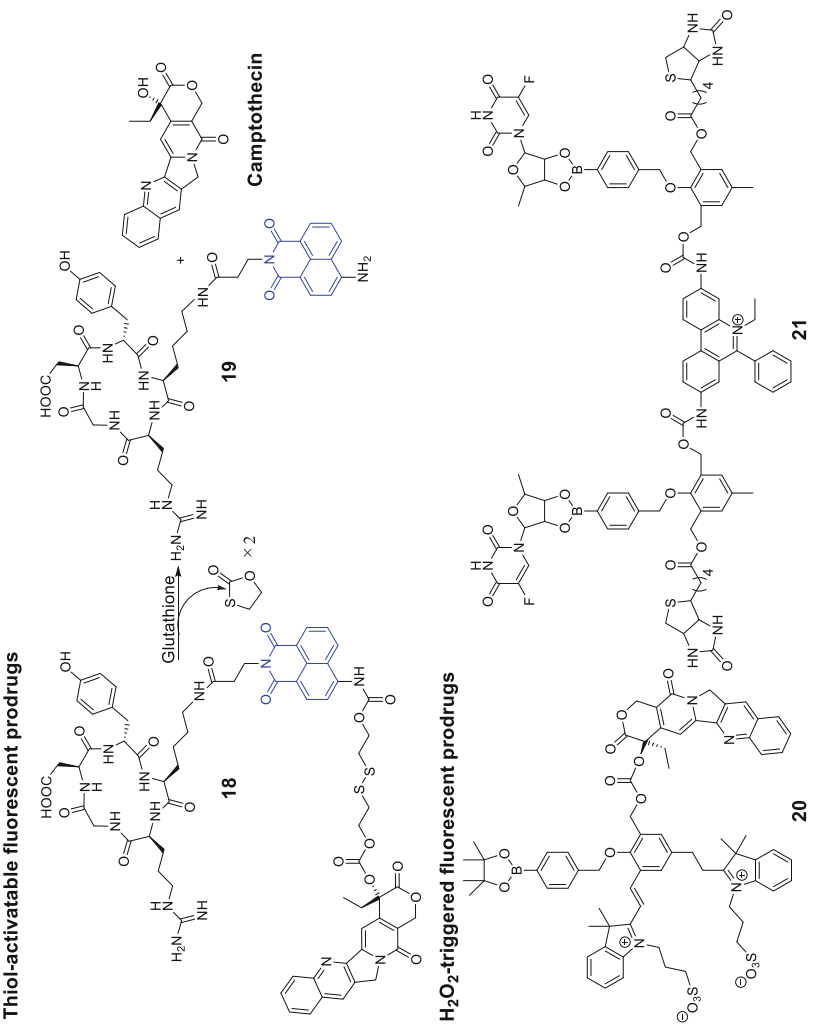

Fig. 19 Representative fluorescent prodrug conjugates

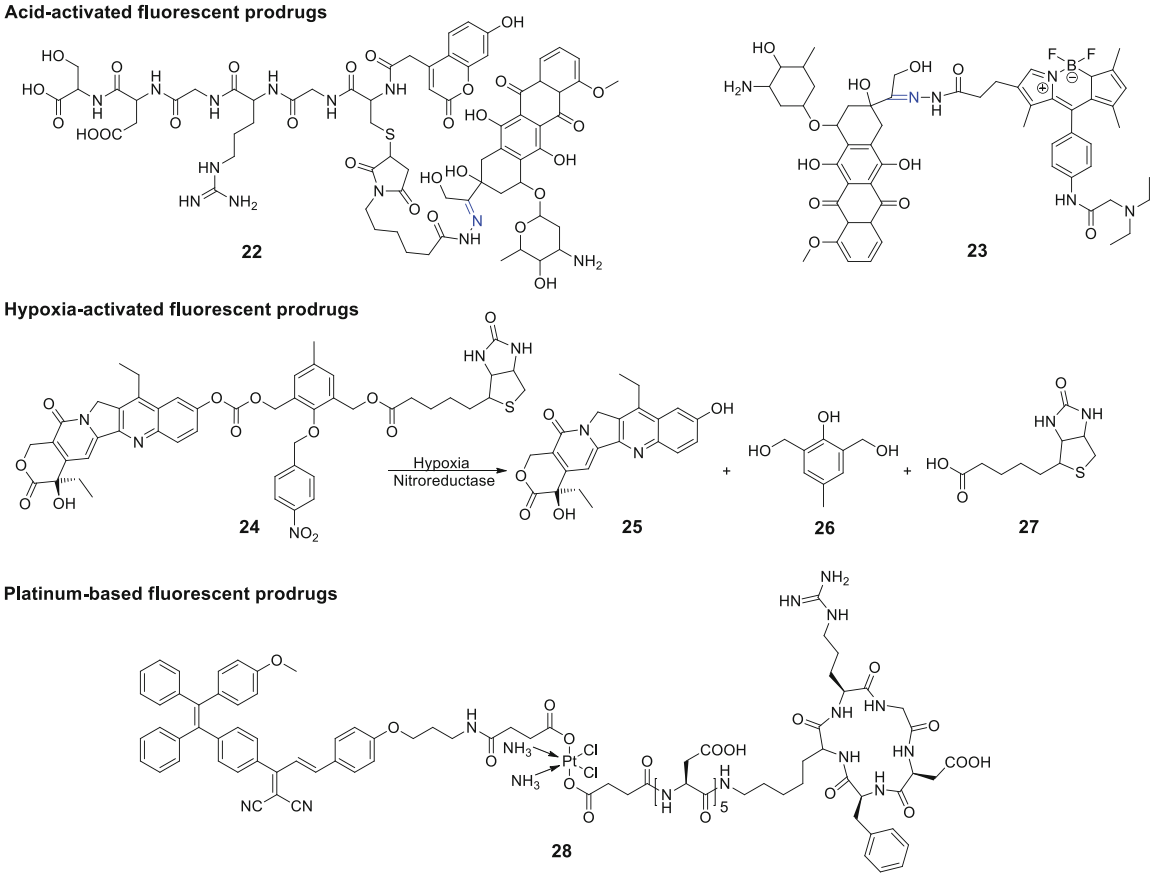

Fig. 19 (continued)

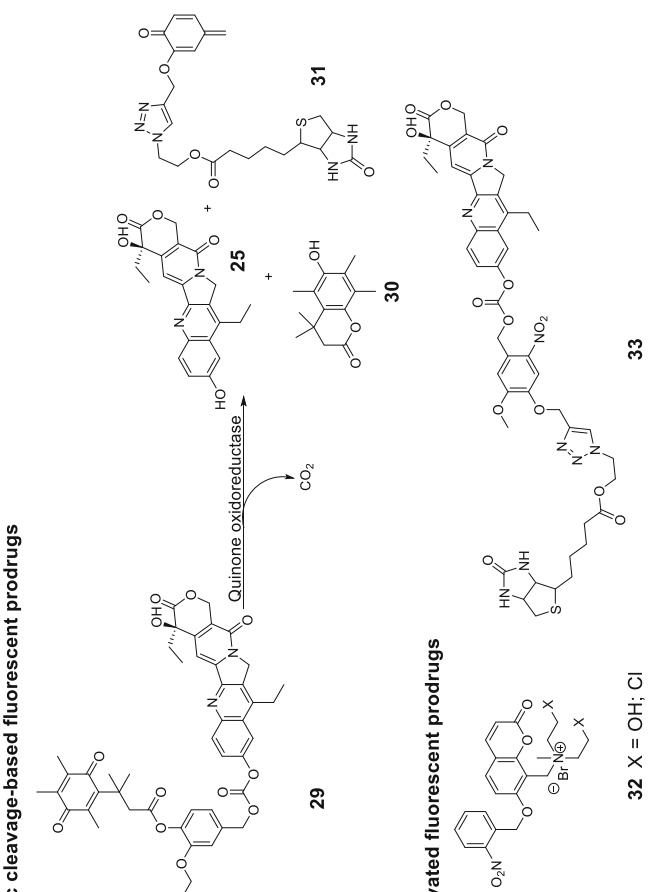

Fig. 19 (continued)

5 Future Perspectives

Currently, FMI has become a powerful and effective tool for drug development. The study of specific probes and targets depends on the development of chemistry and biology, and the FMI tracers do not interfere with the biological process by themselves. The involvement of FMI in metabolic or specific biological processes can more realistically reflect the physiological and pathological processes occurring in organisms, such as gene expression, activation of biochemical pathways, protein interaction, and tracing of cell proliferation and death. Using this noninvasive method to detect cell function can help evaluate the role of new candidate drugs under the influence of complex biological responses in animals. The development of new probes, especially NIR probes, can facilitate the clinical application of this nonradioactive imaging technology. In the last 10 years, FMI has developed rapidly for its low cost, non-ionization, and high throughput, and it plays an important role in all stages of drug development. This technique also has some shortcomings:

1. The detection depth is limited: because of the different wavelengths of the fluorophores and the influence of light absorption and scattering, optical molecular imaging equipment cannot detect cell activity at deeper depths in vivo.
2. Target selection: in order to apply FMI to monitor the efficacy of drug treatment, it is necessary to find specific targets for the diseases. Currently, specific targets of diseases representing the occurrence and development of diseases are not fully discovered.
3. Probe development: the ideal probe should have a high sensitivity and specificity for detection and should not cause an immune response and can be easily cleared by the body. However, the existing FMI probes do not fully meet the above conditions, and the development of new probes is costly.
4. Clinical trials: safety and effectiveness of the application of fluorescence probes in the clinical trials or treatments. In summary, the development of new FMI probes and their application in various stages of drug development will ultimately improve the efficiency of developing new and effective drugs, reduce the cost of research and development, and provide a wider and clinical application prospect in the field of drug development.

Acknowledgments Thanks to Dr. Yang Du, Dr. Chu Tang, and Dr. Yu An for their kind contribution to writing this chapter. This paper is supported by the National Key Research and Development Program of China under Grant Nos. 2017YFA0205200, 2016YFA0201401, 2016YFC0103702, and 2016YFC0102000; the National Natural Science Foundation of China under Grant Nos. 81871514, 81470083, 81227901, 81527805, 61231004, 81601548, and 81772011; the International Innovation Team of CAS under Grant No. 20140491524; and Beijing Municipal Science and Technology Commission No. Z161100002616022.

Compliance with Ethical Standards

Funding: This study was funded by Ministry of Science and Technology of China (grant number 2017YFA0205200, 2017YFA0700401), National Natural Science Foundations of China (grant number 81871514, 81527805), the Strategic Priority Research Program of Chinese Academy of

Sciences (grant number XDB32030200, XDB01030200), and Chinese Academy of Sciences (grant number QYZDJ-SSW-JSC005).

Ethical Approval: This chapter does not contain any studies with human participants or animals performed by any of the authors.

Conflict of Interest: The authors declare no conflict of interest.

References

1. Corrêa IR Jr (2014) Live-cell reporters for fluorescence imaging. Curr Opin Chem Biol 20:36–45
2. Dean KM, Palmer AE (2014) Advances in fluorescence labeling strategies for dynamic cellular imaging. Nat Chem Biol 10(7):512–523
3. Hu Z, Qu Y, Wang K, Zhang X, Zha J, Song T, Bao C, Liu H, Wang Z, Wang J, Liu Z, Liu H, Tian J (2015) In vivo nanoparticle-mediated radiopharmaceutical-excited fluorescence molecular imaging. Nat Commun 6:7560
4. de Jong M, Essers J, van Weerden WM (2014) Imaging preclinical tumour models: improving translational power. Nat Rev Cancer 14(7):481–493
5. Chen X, Wang F, Hyun JY, Wei T, Qiang J, Ren X, Shin I, Yoon J (2016) Recent progress in the development of fluorescent, luminescent and colorimetric probes for detection of reactive oxygen and nitrogen species. Chem Soc Rev 45(10):2976–3016
6. Chi C, Du Y, Ye J, Kou D, Qiu J, Wang J, Tian J, Chen X (2014) Intraoperative imaging-guided cancer surgery: from current fluorescence molecular imaging methods to future multi-modality imaging technology. Theranostics 4(11):1072–1084
7. Gao M, Yu F, Lv C, Choo J, Chen L (2017) Fluorescent chemical probes for accurate tumor diagnosis and targeting therapy. Chem Soc Rev 46(8):2237–2271
8. Jiao X, Li Y, Niu J, Xie X, Wang X, Tang B (2018) Small-molecule fluorescent probes for imaging and detection of reactive oxygen, nitrogen, and sulfur species in biological systems. Anal Chem 90(1):533–555
9. Liu JN, Bu W, Shi J (2017) Chemical design and synthesis of functionalized probes for imaging and treating tumor hypoxia. Chem Rev 117(9):6160–6224
10. Ding F, Zhan Y, Lu X, Sun Y (2018) Recent advances in near-infrared II fluorophores for multifunctional biomedical imaging. Chem Sci 9(19):4370–4380
11. He SQ, Song J, Qu JL, Cheng Z (2018) Crucial breakthrough of second near-infrared biological window fluorophores: design and synthesis toward multimodal imaging and theranostics. Chem Soc Rev 47(12):4258–4278
12. Lavis LD, Raines RT (2014) Bright building blocks for chemical biology. ACS Chem Biol 9 (4):855–866
13. Gonçalves MS (2009) Fluorescent labeling of biomolecules with organic probes. Chem Rev 109(1):190–212
14. Zheng Y, Ji S, Czerwinski A, Valenzuela F, Pennington M, Liu S (2014) FITC-conjugated cyclic RGD peptides as fluorescent probes for staining integrin αvβ3/αvβ5 in tumor tissues. Bioconjug Chem 25(11):1925–1941
15. Bartholomä MD, Gottumukkala V, Zhang S, Baker A, Dunning P, Fahey FH, Treves ST, Packard AB (2012) Effect of the prosthetic group on the pharmacologic properties of 18F-labeled rhodamine B, a potential myocardial perfusion agent for positron emission tomography (PET). J Med Chem 55(24):11004–11012
16. Sun T, Guan X, Zheng M, Jing X, Xie Z (2015) Mitochondria-localized fluorescent BODIPY-platinum conjugate. ACS Med Chem Lett 6(4):430–433
17. Fei XN, Gu YC (2009) Progress in modifications and applications of fluorescent dye probe. Prog Nat Sci 19(1):1–7

18. Qian X, Xu Z (2015) Fluorescence imaging of metal ions implicated in diseases. Chem Soc Rev 44(14):4487–4493
19. Fernández A, Vendrell M (2016) Smart fluorescent probes for imaging macrophageactivity. Chem Soc Rev 45(5):1182–1196
20. Li X, Gao X, Shi W, Ma H (2014) Design strategies for water-soluble small molecular chromogenic and fluorogenic probes. Chem Rev 114(1):590–659
21. Yang Z, Sharma A, Qi J, Peng X, Lee DY, Hu R, Lin D, Qu J, Kim JS (2016) Super-resolution fluorescent materials: an insight into design and bioimaging applications. Chem Soc Rev 45 (17):4651–4667
22. Yang Z, Cao J, He Y, Yang JH, Kim T, Peng X, Kim JS (2014) Macro−/micro-environment-sensitive chemosensing and biological imaging. Chem Soc Rev 43(13):4563–4601
23. Liu K, Kong X, Ma Y, Lin W (2017) Rational design of a robust fluorescent probe for the detection of endogenous carbon monoxide in living zebrafish embryos and mouse tissue. Angew Chem Int Ed Engl 56(43):13489–13492
24. Ling X, Zhang S, Shao P, Li W, Yang L, Ding Y, Xu C, Stella N, Bai M (2015) A novel near-infrared fluorescence imaging probe that preferentially binds to cannabinoid receptors CB2R over CB1R. Biomaterials 57:169–178
25. Deutscher SL (2010) Phage display in molecular imaging and diagnosis of cancer. Chem Rev 110(5):3196–3211
26. Kobayashi H, Ogawa M, Alford R, Choyke PL, Urano Y (2010) New strategies for fluorescent probe design in medical diagnostic imaging. Chem Rev 110(5):2620–2640
27. Smith AM, Mancini MC, Nie S (2009) Bioimaging: second window for in vivo imaging. Nat Nanotechnol 4(11):710–7111
28. Hong G, Diao S, Antaris AL, Dai H (2015) Carbon nanomaterials for biological imaging and nanomedicinal therapy. Chem Rev 115(19):10816–10906
29. Welsher K, Liu Z, Sherlock SP, Robinson JT, Chen Z, Daranciang D, Dai H (2009) A route to brightly fluorescent carbon nanotubes for near-infrared imaging in mice. Nat Nanotechnol 4 (11):773–780
30. Diao S, Blackburn JL, Hong G, Antaris AL, Chang J, Wu JZ, Zhang B, Cheng K, Kuo CJ, Dai H (2015) Fluorescence imaging in vivo at wavelengths beyond 1500 nm. Angew Chem Int Ed Engl 54(49):14758–14762
31. Antaris AL, Chen H, Cheng K, Sun Y, Hong G, Qu C, Diao S, Deng Z, Hu X, Zhang B, Zhang X, Yaghi OK, Alamparambil ZR, Hong X, Cheng Z, Dai HJ (2016) A small-molecule dye for NIR-II imaging. Nat Mater 15(2):235–242
32. Jiang YX, Ding BB, Xiao YL, Xing L, Hong XC, Cheng Z (2016) Novel benzo-bis(1,2,5-thiadiazole) fluorophores for in vivo NIR-II imaging of cancer. Chem Sci 7(9):6203–6207
33. Yang Q, Hu Z, Zhu S, Ma R, Ma H, Ma Z, Wan H, Zhu T, Jiang Z, Liu W, Jiao L, Sun H, Liang Y, Dai H (2018) Donor engineering for NIR-II molecular fluorophores with enhanced fluorescent performance. J Am Chem Soc 140(5):1715–1724
34. Céspedes-Guirao FJ, Ropero AB, Font-Sanchis E, Nadal Á, Fernández-Lázaro F, Sastre-Santo Á (2011) A water-soluble perylene dye functionalised with a 17β-estradiol: a new fluorescent tool for steroid hormones. Chem Commun 47(29):8307–8309
35. Rickert EL, Oriana S, Hartman-Frey C, Long X, Webb TT, Nephew KP, Weatherman RV (2010) Synthesis and characterization of fluorescent 4-hydroxytamoxifen conjugates with unique antiestrogenic properties. Bioconjug Chem 21(5):903–910
36. Yang L, Hu ZY, Luo JJ, Tang C, Zhang SL, Ning WT, Dong C, Huang J, Liu XJ, Zhou HB (2017) Dual functional small molecule fluorescent probes for image-guided estrogen receptor-specific targeting coupled potent antiproliferative potency for breast cancer therapy. Bioorg Med Chem 25(13):3531–3539
37. Levi J, Cheng Z, Gheysens O, Patel M, Chan CT, Wang Y, Namavari M, Gambhir SS (2007) Fluorescent fructose derivatives for imaging breast cancer cells. Bioconjug Chem 18 (3):628–634

38. Humblet V, Lapidus R, Williams LR, Tsukamoto T, Rojas C, Majer P, Hin B, Ohnishi S, De Grand AM, Zaheer A, Renze JT, Nakayama A, Slusher BS, Frangioni JV (2005) High-affinity near-infrared fluorescent small-molecule contrast agents for in vivo imaging of prostate-specific membrane antigen. Mol Imaging 4(4):448–462
39. Liu T, Wu LY, Kazak M, Berkman CE (2008) Cell-surface labeling and internalization by a fluorescent inhibitor of prostate-specific membrane antigen. Prostate 68(9):955–964
40. Liu T, Wu LY, Hopkins MR, Choi JK, Berkman CE (2010) A targeted low molecular weight near-infrared fluorescent probe for prostate cancer. Bioorg Med Chem Lett 20(23):7124–7126
41. Baranski AC, Schäfer M, Bauder-Wüst U, Roscher M, Schmidt J, Stenau E, Simpfendörfer T, Teber D, Maier-Hein L, Hadaschik B, Haberkorn U, Eder M, Kopka K (2018) PSMA-11-derived dual-labeled PSMA inhibitors for preoperative PET imaging and precise fluorescence-guided surgery of prostate cancer. J Nucl Med 59(4):639–645
42. Kennedy MD, Jallad KN, Thompson DH, Ben-Amotz D, Low PS (2003) Optical imaging of metastatic tumors using a folate-targeted fluorescent probe. J Biomed Opt 8(4):636–641
43. van Dam GM, Themelis G, Crane LM, Harlaar NJ, Pleijhuis RG, Kelder W, Sarantopoulos A, de Jong JS, Arts HJ, van der Zee AG, Bart J, Low PS, Ntziachristos V (2011) Intraoperative tumor-specific fluorescence imaging in ovarian cancer by folate receptor-α targeting: first in-human results. Nat Med 17(10):1315–1319
44. Uddin MJ, Crews BC, Blobaum AL, Kingsley PJ, Gorden DL, McIntyre JO, Matrisian LM, Subbaramaiah K, Dannenberg AJ, Piston DW, Marnett LJ (2010) Selective visualization of cyclooxygenase-2 in inflammation and cancer by targeted fluorescent imaging agents. Cancer Res 70(9):3618–3627
45. Zhang H, Fan J, Wang J, Dou B, Zhou F, Cao J, Qu J, Cao Z, Zhao W, Peng X (2013) Fluorescence discrimination of cancer from inflammation by molecular response to COX-2 enzymes. J Am Chem Soc 135(46):17469–17475
46. Krall N, Pretto F, Decurtins W, Bernardes GJ, Supuran CT, Neri D (2014) A small-molecule drug conjugate for the treatment of carbonic anhydrase IX expressing tumors. Angew Chem Int Ed Engl 53(16):4231–4235
47. Krall N, Pretto F, Neri D (2014) A bivalent small molecule-drug conjugate directed against carbonic anhydrase IX can elicit complete tumour regression in mice. Chem Sci 5:3640–3644
48. Chenouard N, Smal I, de Chaumont F, Maška M, Sbalzarini IF, Gong Y, Cardinale J, Carthel C, Coraluppi S, Winter M, Cohen AR, Godinez WJ, Rohr K, Kalaidzidis Y, Liang L, Duncan J, Shen H, Xu Y, Magnusson KE, Jaldén J, Blau HM, Paul-Gilloteaux P, Roudot P, Kervrann C, Waharte F, Tinevez JY, Shorte SL, Willemse J, Celler K, van Wezel GP, Dan HW, Tsai YS, Ortiz de Solórzano C, Olivo-Marin JC, Meijering E (2014) Nat Methods 11(3):281–289
49. Xie W, Deng Y, Wang K, Yang X, Luo Q (2014) Reweighted L1 regularization for restraining artifacts in FMT reconstruction images with limited measurements. Opt Lett 39 (14):4148–4151
50. Qin CH, Feng JC, Zhu SP, Ma XB, Zhong JH, Wu P, Jin ZY, Tian J (2014) Recent advances in bioluminescence tomography: methodology and system as well as application. Laser Photonics Revs 8(1):94–114
51. Wang K, Wang Q, Luo Q, Yang X (2015) Fluorescence molecular tomography in the second near-infrared window. Opt Express 23(10):12669–12679
52. Leng CC, Tian J (2015) Mathematical method in optical molecular imaging. Sci China Inf Sci 58(3):1–13
53. Zhang S, Wang K, Liu HB, Leng CC, Gao Y, Tian J (2017) Reconstruction method for in vivo bioluminescence tomography based on the split Bregman iterative and surrogate functions. Mol Imaging Biol 19(2):245–255
54. Fan-Minogue H, Cao Z, Paulmurugan R, Chan CT, Massoud TF, Felsher DW, Gambhir SS (2010) Noninvasive molecular imaging of c-Myc activation in living mice. Proc Natl Acad Sci U S A 107(36):15892–15897

55. van Dam GM, Themelis G, Crane LM, Harlaar NJ, Pleijhuis RG, Kelder W, Sarantopoulos A, de Jong JS, Arts HJ, van der Zee AG, Bart J, Low PS, Ntziachristos V (2011) Intraoperative tumor-specific fluorescence imaging in ovarian cancer by folate receptor-alpha targeting: first in-human results. Nat Med 17(10):1315–1319
56. Whitney MA, Crisp JL, Nguyen LT, Friedman B, Gross LA, Steinbach P, Tsien RY, Nguyen QT (2011) Fluorescent peptides highlight peripheral nerves during surgery in mice. Nat Biotechnol 29(4):352–356
57. Solomon B, Cornelis F (2016) Interventional molecular imaging. J Nucl Med 57(4):493–496
58. Tarvainen T, Vauhkonen M, Kolehmainen V, Kaipio JP (2005) Hybrid radiative-transfer-diffusion model for optical tomography. Appl Optics 44(6):876–886
59. Tualle JM, Tinet E (2003) Derivation of the radiative transfer equation for scattering media with a spatially varying refractive index. Opt Commun 228(1–3):33–38
60. Song X, Wang D, Chen N, Bai J, Wang H (2007) Reconstruction for free-space fluorescence tomography using a novel hybrid adaptive finite element algorithm. Opt Express 15 (26):18300–18317
61. Han D, Yang X, Liu K, Qin C, Zhang B, Ma X, Tian J (2010) Efficient reconstruction method for L1 regularization in fluorescence molecular tomography. Appl Optics 49(36):6930–6937
62. Hyde D, Miller EL, Brooks DH, Ntziachristos V (2010) Data specific spatially varying regularization for multimodal fluorescence molecular tomography. IEEE Trans Med Imaging 29(2):365–374
63. Guo X, Liu X, Wang X, Tian F, Liu F, Zhang B, Hu G, Bai J (2010) A combined fluorescence and microcomputed tomography system for small animal imaging. IEEE Trans Biomed Eng 57(12):2876–2883
64. Zhang B, Yang X, Qin C, Liu D, Zhu S, Feng J, Sun L, Liu K, Han D, Ma X, Zhang X, Zhong J, Li X, Yang X, Tian J (2010) A trust region method in adaptive finite element framework for bioluminescence tomography. Opt Express 18(7):6477–6491
65. Lin Y, Kwong TC, Bolisay L, Gulsen G (2012) Temperature-modulated fluorescence tomography based on both concentration and lifetime contrast. J Biomed Opt 17(5):056007
66. Han D, Tian J, Liu K, Feng J, Zhang B, Ma X, Qin C (2010) Sparsity-promoting tomographic fluorescence imaging with simplified spherical harmonics approximation. IEEE Trans Biomed Eng 57(10):2564–2567
67. Aydin ED, de Oliveira CR, Goddard AJ (2002) A comparison between transport and diffusion calculations using a finite element-spherical harmonics radiation transport method. Med Phys 29(9):2013–2023
68. Khan T, Thomas A (2005) Comparison of P-N or spherical harmonics approximation for scattering media with spatially varying and spatially constant refractive indices. Opt Commun 255(1–3):130–166
69. Klose AD, Larsen EW (2006) Light transport in biological tissue based on the simplified spherical harmonics equations. J Comput Phys 220(1):441–470
70. Klose AD (2010) The forward and inverse problem in tissue optics based on the radiative transfer equation: a brief review. J Quant Spectrosc Radiat Transf 111(11):1852–1853
71. Grella K, Schwab C (2011) Sparse tensor spherical harmonics approximation in radiative transfer. J Comput Phys 230(23):8452–8473
72. Duderstadt JJ, Martin WR (1979) Transport theory. Wiley, New York
73. Arridge SR, Hebden JC (1997) Optical imaging in medicine: II. Modelling and reconstruction. Phys Med Biol 42(5):841–853
74. Cong W, Wang G (2006) Boundary integral method for bioluminescence tomography. J Biomed Opt 11(2):020503
75. Qin C, Tian J, Yang X, Liu K, Yan G, Feng J, Lv Y, Xu M (2008) Galerkin-based meshless methods for photon transport in the biological tissue. Opt Express 16(25):20317–20333
76. Wright S, Schweiger M, Arridge SR (2007) Reconstruction in optical tomography using the PN approximations. Meas Sci Technol 18(18):79–86

77. Lu Y, Zhang X, Douraghy A, Stout D, Tian J, Chan TF, Chatziioannou AF (2009) Source reconstruction for spectrally-resolved bioluminescence tomography with sparse a priori information. Opt Express 17(10):8062–8080
78. An Y, Liu J, Zhang G, Jiang S, Ye J, Chi C, Tian J (2017) Compactly supported radial basis function-based meshless method for photon propagation model of fluorescence molecular tomography. IEEE Trans Med Imaging 36(2):366–373
79. Zhu W, Wang Y, Yao Y, Chang J, Graber HL, Barbour RL (1997) Iterative total least-squares image reconstruction algorithm for optical tomography by the conjugate gradient method. J Opt Soc Am A Opt Image Sci Vis 14(4):799–807
80. Paulsen KD, Jiang H (1996) Enhanced frequency-domain optical image reconstruction in tissues through total-variation minimization. Appl Optics 35(19):3447–3458
81. Yu DF, Fessler JA (1998) Edge-preserving tomographic reconstruction with nonlocal regularization. IEEE Trans Med Imaging 21(2):159–173
82. Darne C, Lu Y, Sevick-Muraca EM (2014) Small animal fluorescence and bioluminescence tomography: a review of approaches, algorithms and technology update. Phys Med Biol 59(1): R1–R64
83. Han D, Tian J, Zhu S, Feng J, Qin C, Zhang B, Yang X (2010) A fast reconstruction algorithm for fluorescence molecular tomography with sparsity regularization. Opt Express 18 (8):8630–8646
84. Zacharakis G, Kambara H, Shih H, Ripoll J, Grimm J, Saeki Y, Weissleder R, Ntziachristos V (2005) Volumetric tomography of fluorescent proteins through small animals in vivo. Proc Natl Acad Sci U S A 102(51):18252–18257
85. Ntziachristos V (2010) Going deeper than microscopy: the optical imaging frontier in biology. Nat Methods 7(8):603–614
86. Ale A, Ermolayev V, Herzog E, Cohrs C, de Angelis MH, Ntziachristos V (2012) FMT-XCT: in vivo animal studies with hybrid fluorescence molecular tomography-X-ray computed tomography. Nat Methods 9(6):615–620
87. Mohajerani P, Hipp A, Willner M, Marschner M, Trajkovic-Arsic M, Ma X, Burton NC, Klemm U, Radrich K, Ermolayev V, Tzoumas S, Siveke JT, Bech M, Pfeiffer F, Ntziachristos V (2014) FMT-PCCT: hybrid fluorescence molecular tomography-x-ray phase-contrast CT imaging of mouse models. IEEE Trans Med Imaging 33(7):1434–1446
88. Mohajerani P, Ntziachristos V (2016) An inversion scheme for hybrid fluorescence molecular tomography using a fuzzy inference system. IEEE Trans Med Imaging 35(2):381–390
89. Berninger MT, Mohajerani P, Kimm M, Masius S, Ma X, Wildgruber M, Haller B, Anton M, Imhoff AB, Ntziachristos V, Henning TD, Meier R (2017) Fluorescence molecular tomography of DiR-labeled mesenchymal stem cell implants for osteochondral defect repair in rabbit knees. Eur Radiol 27(3):1105–1113
90. Allard M, Côté D, Davidson L, Dazai J, Henkelman RM (2007) Combined magnetic resonance and bioluminescence imaging of live mice. J Biomed Opt 12(3):034018
91. Cao X, Yang J, Gao Y, Guo Y, Wu G, Shen D (2017) Dual-core steered non-rigid registration for multi-modal images via bi-directional image synthesis. Med Image Anal 41:18–31
92. Phillips EH, Di Achille P, Bersi MR, Humphrey JD, Goergen CJ (2017) Multi-modality imaging enables detailed hemodynamic simulations in dissecting aneurysms in mice. IEEE Trans Med Imaging 36(6):1297–1305
93. Chen ZY, Wang YX, Yang F, Lin Y, Zhou QL, Liao YY (2014) New researches and application progress of commonly used optical molecular imaging technology. Biomed Res Int 2014:429198
94. Zhang Y, Zhang B, Liu F, Luo J, Bai J (2014) In vivo tomographic imaging with fluorescence and MRI using tumor-targeted dual-labeled nanoparticles. Int J Nanomedicine 9:33–41
95. Wang K, Chi CW, Hu ZH, Liu MH, Hui H, Shang WT, Peng D, Zhang S, Ye JZ, Liu HX, Tian J (2015) Optical molecular imaging frontiers in oncology: the pursuit of accuracy and sensitivity. Engineering 1(3):309–323

96. An Y, Liu J, Zhang G, Ye J, Du Y, Mao Y, Chi C, Tian J (2015) A novel region reconstruction method for fluorescence molecular tomography. IEEE Trans Biomed Eng 62(7):1818–1826
97. Zhang J, Shi J, Guang H, Zuo S, Liu F, Bai J, Luo J (2016) Iterative correction scheme based on discrete cosine transform and L1 regularization for fluorescence molecular tomography with background fluorescence. IEEE Trans Biomed Eng 63(6):1107–1115
98. Pera V, Brooks DH, Niedre M (2016) Multiplexed fluorescence tomography with spectral and temporal data: demixing with intrinsic regularization. Biomed Opt Express 7(1):111–131
99. Lian L, Deng Y, Xie W, Xu G, Yang X, Zhang Z, Luo Q (2016) High-dynamic-range fluorescence molecular tomography for imaging of fluorescent targets with large concentration differences. Opt Express 24(17):19920–19933
100. Zhang G, Liu F, Liu J, Luo J, Xie Y, Bai J, Xing L (2017) Cone beam X-ray luminescence computed tomography based on bayesian method. IEEE Trans Med Imaging 36(1):225–235
101. Zhou Y, Chen M, Su H, Luo J (2017) Self-prior strategy for organ reconstruction in fluorescence molecular tomography. Biomed Opt Express 8(10):4671–4686
102. Shi J, Udayakumar TS, Wang Z, Dogan N, Pollack A, Yang Y (2017) Optical molecular imaging-guided radiation therapy part 2: integrated x-ray and fluorescence molecular tomography. Med Phys 44(9):4795–4803
103. Baikejiang R, Zhao Y, Fite BZ, Ferrara KW, Li C (2017) Anatomical image-guided fluorescence molecular tomography reconstruction using kernel method. J Biomed Opt 22(5):055001
104. He X, Wang X, Yi H, Chen Y, Zhang X, Yu J, He X (2017) Laplacian manifold regularization method for fluorescence molecular tomography. J Biomed Opt 22(4):45009
105. Dutta J, Ahn S, Li C, Cherry SR, Leahy RM (2012) Joint L1 and total variation regularization for fluorescence molecular tomography. Phys Med Biol 57(6):1459–1476
106. Meng Q, Liu Z, Li F, Ma J, Wang H, Huan Y, Li Z (2015) An HDAC-targeted imaging probe LBH589-Cy5.5 for tumor detection and therapy evaluation. Mol Pharm 12(7):2469–2476
107. Hu ZY, Yang L, Ning W, Tang C, Meng Q, Zheng J, Dong C, Zhou HB (2018) A high-affinity subtype-selective fluorescent probe for estrogen receptor β imaging in living cells. Chem Commun 54(31):3887–3890
108. McCann TE, Kosaka N, Mitsunaga M, Choyke PL, Gildersleeve JC, Kobayashi H (2010) Biodistribution and excretion of monosaccharide-albumin conjugates measured with in vivo near-infrared fluorescence imaging. Bioconjug Chem 21(10):1925–1932
109. Kumar R, Shin WS, Sunwoo K, Kim WY, Koo S, Bhuniya S, Kim JS (2015) Small conjugate-based theranostic agents: an encouraging approach for cancer therapy. Chem Soc Rev 44 (19):6670–6683
110. Lim EK, Kim T, Paik S, Haam S, Huh YM, Lee K (2015) Nanomaterials for theranostics: recent advances and future challenges. Chem Rev 115(1):327–394
111. Lee MH, Yang Z, Lim CW, Lee YH, Dongbang S, Kang C, Kim JS (2013) Disulfide-cleavage-triggered chemosensors and their biological applications. Chem Rev 113(7):5071–5109
112. Lee MH, Sharma A, Chang MJ, Lee J, Son S, Sessler JL, Kang C, Kim JS (2018) Fluorogenic reaction-based prodrug conjugates as targeted cancer theranostics. Chem Soc Rev 47(1):28–52
113. Wong PT, Choi SK (2015) Mechanisms of drug release in nanotherapeutic delivery systems. Chem Rev 115(9):3388–3432
114. Lee MH, Kim JY, Han JH, Bhuniya S, Sessler JL, Kang C, Kim JS (2012) Direct fluorescence monitoring of the delivery and cellular uptake of a cancer-targeted RGD peptide-appended naphthalimide theranostic prodrug. J Am Chem Soc 134(30):12668–12674
115. Redy-Keisar O, Ferber S, Satchi-Fainaro R, Shabat D (2015) NIR fluorogenic dye as a modular platform for prodrug assembly: real-time in vivo monitoring of drug release. ChemMedChem 10(6):999–1007
116. Kumar R, Han J, Lim HJ, Ren WX, Lim JY, Kim JH, Kim JS (2014) Mitochondrial induced and self-monitored intrinsic apoptosis by antitumor theranostic prodrug: in vivo imaging and precise cancer treatment. J Am Chem Soc 136(51):17836–17843

117. Li SY, Liu LH, Jia HZ, Qiu WX, Rong L, Cheng H, Zhang XZ (2014) A pH-responsive prodrug for real-time drug release monitoring and targeted cancer therapy. Chem Commun 50 (80):11852–11855
118. Fernandez A, Vermeren M, Humphries D, Subiros-Funosas R, Barth N, Campana L, MacKinnon A, Feng Y, Vendrell M (2017) Chemical modulation of in vivo macrophage function with subpopulation-specific fluorescent prodrug conjugates. ACS Cent Sci 3 (9):995–1005
119. Kumar R, Kim EJ, Han J, Lee H, Shin WS, Kim HM, Bhuniya S, Kim JS, Hong KS (2016) Hypoxia-directed and activated theranostic agent: imaging and treatment of solid tumor. Biomaterials 104:119–128
120. Yuan Y, Zhang CJ, Liu B (2015) A platinum prodrug conjugated with a photosensitizer with aggregation-induced emission (AIE) characteristics for drug activation monitoring and combinatorial photodynamic-chemotherapy against cisplatin resistant cancer cells. Chem Commun 51(41):8626–8629
121. Shin WS, Han J, Verwilst P, Kumar R, Kim JH, Kim JS (2016) Cancer targeted enzymatic theranostic prodrug: precise diagnosis and chemotherapy. Bioconjug Chem 27(5):1419–1426
122. Cao Y, Pan R, Xuan W, Wei Y, Liu K, Zhou J, Wang W (2015) Photo-triggered fluorescent theranostic prodrugs as DNA alkylating agents for mechlorethamine release and spatiotemporal monitoring. Org Biomol Chem 13(24):6742–6748